Nanoparticle Oscillators

DOI: 10.1002/ange.201004231

Nanoparticle Oscillations and Fronts**

*István Lagzi, Bartlomiej Kowalczyk, Dawei Wang, and Bartosz A. Grzybowski**

Self-organization outside the thermodynamic equilibrium is important in the context of life,[1,2] and has inspired development of artificial dynamic materials and systems[3,4] on scales from molecular,[5–9] through nanoscopic[10–12] and microscopic,[13,14] to macroscopic.[15,16] One of the singular features of non-equilibrium self-organization in cells or organisms is their ability to couple several subsystems into larger, dynamic machinery.[2] In man-made ensembles, such synthetic ability is largely lacking, though there are some interesting examples where molecular-scale, non-equilibrium systems such as chemical oscillators control dimensions/contractility of gels or polymers[17,18] or periodically shift complexation or precipitation equilibria.[19–22] The motivation of the present work is to design and implement a chemical system in which a molecular-scale subsystem would couple to and control dynamic self-organization of nanoscopic part.[23] This subsystem is a pH oscillator[24–26] (pH "clock") that controls the dissociation of acidic head-groups on the surface of metal nanoparticles (NPs). We show that with a proper control over electrostatic and van der Waals (vdW) forces between the NPs,[27] the clock can then cause a rhythmic assembly/disassembly of the NPs. Additionally, in spatially distributed media, the pH oscillations can translate into the propagation of NP aggregation fronts or surface phenomena, such as deposition and removal of NP-based surface coatings.

Although conceptually straightforward (Figure 1a), the ability to couple pH oscillations with reversible NP aggregation requires careful engineering of the interparticle forces at a molecular scale. The two key effects to consider are the vdW attractions between the NPs and the electrostatic repulsions between the molecules forming self-assembled monolayers (SAMs)[28,29] on nanoparticle surfaces. Specifically, when the pH clock "spikes" to high pH and deprotonates the SAMs, the electrostatic repulsions should be able to overcome vdW attractions; conversely, when the oscillator is in a low-pH state, the vdW forces should be strong enough to affect NP aggregation. To match these criteria, 1) the pK_a of the SAMs covering the NPs should be within the pH range of the oscillator (such that the oscillations can significantly affect the fractions of protonated/deprotonated molecules within the SAM, and 2) the magnitudes of electrostatic and vdW forces acting in the system should be commensurate; as we have shown previously,[30] the second point is true for NPs that are a few nanometers in diameter, for which the magnitudes of electrostatic and vdW interactions are on the order of several kT.[31] As the interaction energies are relatively small, the aggregation/dispersion phenomena might be expected to be sensitive to the thickness of the SAMs (determining the distance between the NPs metal cores and thus the maximal magnitude of vdW interactions between the particles).[27]

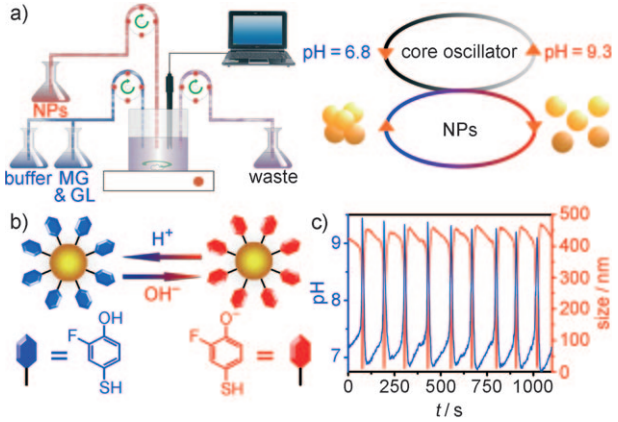

Figure 1. Nanoparticle oscillators. a) The experimental setup and the coupling of the pH oscillator to NP aggregation/dispersion. MG = methylene glycol, GL = gluconolactone. b) Au NPs coated with 2-fluoro *para*-mercaptophenol (FMP) ligands. Blue: low pH, protonated; red: high pH, deprotonated. c) Oscillations in pH and in NP aggregation are in-phase. Blue curve: solution pH; red: size of the NP aggregates measured concurrently by dynamic light scattering.

With these design guidelines in mind, we considered a system based on the so-called methylene glycol/sulfite/gluconolactone (MGSG) oscillator.[24–26] Our choice was motivated by the fact that this oscillator covers a relatively broad range of pH (ca. 6.8 to ca. 9.3) and is based on simple chemical reactions that are not expected to interfere with typical SAMs. We then tested Au and/or Ag NPs with average diameters in different samples $d = 6.5$–10 nm (standard deviations: $\sigma = 10$–$15\,\%$) and functionalized with alkane thiolates terminated in acidic groups; for example, mercaptoundecanoic acid, MUA (pK_a in solution ca. 4.8, pK_a in a SAM reported between 6 and 8;[32] *para*-mercaptophenol, (pK_a in solution ca. 9.3[33]); and 2-fluoro *para*-mercaptophenol, FMP

[*] Dr. I. Lagzi,[+] Dr. B. Kowalczyk,[+] D. Wang, Prof. B. A. Grzybowski
Department of Chemical and Biological Engineering
Department of Chemistry, Northwestern University
2145 Sheridan Rd., Evanston, IL 60208 (USA)
E-mail: grzybor@northwestern.edu
Homepage: http://dysa.northwestern.edu

D. Wang
School of Materials Science and Engineering
Northwestern Polytechnical University
Xi'an 710072 (China)

[+] These authors contributed equally to this work.

[**] The authors thank Dr. Klára Kovács for many helpful discussions. This work was supported by the DARPA program (01-130130-00//W911NF-08-1-0143) and the Non-equilibrium Energy Research Center, which is an Energy Frontier Research Center funded by the U.S. Department of Energy, Office of Science, Office of Basic Energy Sciences under Award Number DE-SC0000989.

Supporting information for this article is available on the WWW under http://dx.doi.org/10.1002/anie.201004231.

($pK_a \approx 8.3$;[34] Figure 1b). The NPs stabilized with mercaptoundecanoic acid did not aggregate at all over the pH range of the oscillator, which is most likely because majority of MUA ligands are deprotonated over this range and the interparticle repulsions are strong; at the same time, the vdW attractions between the metal cores are weak (because MUA SAMs are relatively thick: ca. 1.6 nm). The opposite behavior was observed with NPs stabilized with *para*-mercaptophenol SAMs. In this case, the particles remained aggregated over the entire pH range; this behavior could be attributed to the fact that for this high-pK_a ligand, the electrostatic repulsions are weak whereas vdW attractions are relatively strong (because the SAM is only about 0.5 nm thick). Oscillatory aggregation was observed only in systems comprising NPs functionalized with 2-fluoro *para*-mercaptophenol.

Most experiments were performed in a continuously stirred tank reactor (CSTR) configuration, in which reactants are fed and products removed continuously and oscillations can be sustained indefinitely (Figure 1a). Specifically, 10–30 mM solutions (in terms of metal atoms) of Au/FMP or Ag/FMP NPs were flowed into a 10 mL CSTR at 0.06 mL min^{-1}. Concurrently, two other solutions (constituting the components of the MGSG pH oscillator)[24–26] were fed through the reactor at 1.52 mL min^{-1}: 1) sodium sulfite/sodium bisulfite buffer ($[SO_3^{2-}] = 0.01$M, $[HSO_3^-] = 0.1$M), and 2) a solution of formaldehyde (0.2 M) and gluconolactone (0.0134 M). The pH in the reactor was monitored by a pH electrode (Metler Toledo), and the temperature was kept constant at (22.0 ± 0.2) °C.

The key feature of this system is that the pK_a of the FMP ligands on the NPs falls within the pH range of 6.8–9.3 for the MGSG oscillator (Figure 1c). Consequently, when the oscillator is in the low-pH state, the majority of the ligands are protonated and the electrostatic repulsions between the NPs are weak; under such circumstances, the interparticle interactions are dominated by van der Waals attractions, and the NPs aggregate. When, however, the oscillator "spikes" to pH ≈ 9.3, the ligands become deprotonated (zeta potential decreases from about −40 mV to −50 mV) and the charge–charge interparticle repulsions cause the particles to disperse. In other words, the chemical pH oscillations translate into and are in-phase with the rhythmic aggregation/dispersion of the NPs (Figure 1c). These NP oscillations manifest themselves in pronounced color changes (Figure 2; Supporting Information, Movies 1 and 2), which are due to the electrodynamic coupling[35,36] between the aggregated NPs (when NP cores are separated only by the SAMs; ca. 1 nm) and lack of such coupling between dispersed particles (when the average distance between NPs is over 100 nm). The specific colors depend on the nature of the nanoparticle metal cores. For example, solutions containing AuFMP NPs oscillate between purple and red (Figure 2a) reflecting the positions of the surface plasmon resonance (SPR) band ($\lambda^{agg}_{max,Au} = 563$ nm for NP aggregates and $\lambda^{free}_{max,Au} = 523$ nm for free particles). Silver-based systems change color from dark yellow ($\lambda^{agg}_{max,Au} =$ 460 nm) to light yellow ($\lambda^{free}_{max,Au} = 429$ nm; Figure 2b). An interesting optical behavior is seen in oscillators comprising both AuFMP and AgFMP NPs (Figure 2c; Supporting Information, Movie 3). For the free NPs, the SPR band of

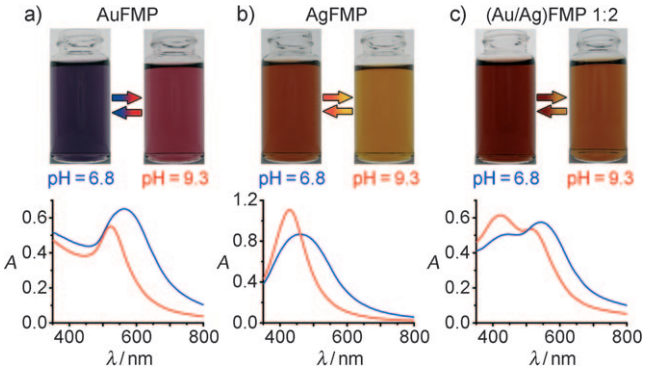

Figure 2. Color changes in various types of NP oscillators. In all cases, the metal cores of the NPs are coated with FMP ligands. a–c) Upper: Oscillators based on a 0.2 mM solution of (6.4 ± 0.9) nm Au NPs (a); a 0.2 mM solution of (6.5 ± 1.0) nm Ag NPs (b); and a mixture of 0.067 mM Au NPs and 0.133 mM Ag NPs (c). Below: UV/Vis spectra corresponding to the low- and high-pH states of the oscillators shown in (a–c).

AgFMP NPs at 424 nm is stronger than that of AuFMP NPs at about 520 nm. When, however, the NPs aggregate, the Au band at about 544 nm becomes more intense. This effect is due to the fact that the resonant frequency of aggregated AgFMP NPs is shifted to longer wavelength by the nearby Au NPs in the aggregate.[30,32,36] We note that for all NP types, the observed colors do not change perceptibly when NP concentrations change (as electrodynamic coupling is mostly due to near-neighbor interactions in the NP aggregates[35–37]), but the sizes of the aggregates increase with nanoparticle concentration, (for example, ca. 300 nm for 0.02 mM NP solutions, ca. 500 nm for 0.2 mM, and ca. 800 nm for 2 mM).

The NPs oscillate rather than irreversibly clump together because the electrostatic interparticle repulsions induced by the high-pH state of the MGSG oscillator can compete effectively with the always-present vdW attractions between the particles. To show this, we consider pairwise[37] NP–NP interactions acting in the system. The interparticle vdW energy[27,30] is given by Equation (1):

$$u_{vdW} = -\frac{A}{3}\left[\frac{R_c^2}{d^2 - 4R_c^2} + \frac{R_c^2}{d^2} + \frac{1}{2}\ln\left(1 - \frac{4R_c^2}{d^2}\right)\right] \quad (1)$$

where $A = 4 \times 10^{-19}$ J is the Hamaker constant for gold across water,[38] R_c is the radius of the metal core, and $d = 2R + h = 2(R_c + \delta) + h$ is the distance between centers of two NPs, where R is the radius of SAM-covered NP, δ is the SAM thickness, and h is the distance of closest approach between two NPs. Electrostatic interactions between charged NPs in ionic solution are derived from the appropriate electrostatic potentials, ϕ, by thermodynamic integration, and, unlike simple DLVO model,[39] account for charge regulation at the surfaces of the NP.[27,30] Following electrostatic calculations (Supporting Information, Section 1), the vdW, electrostatic, and total interaction potentials can be calculated for different pH values. Figure 3a shows that for the low-pH state of the oscillator (pH 6.8), the net interaction between the NPs is dominated by the vdW forces and is attractive; that is,

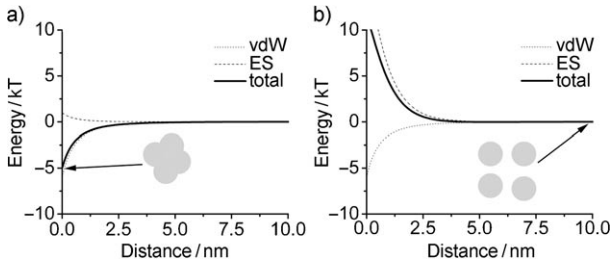

Figure 3. Calculated interaction potentials between a) aggregating Au NPs at pH 6.8 and b) dispersing Au NPs at pH 9, where $u_{total}(h) = u_{vdW}(h) + u_{ES}(h)$. (Other parameters: $R_c = 3.25$ nm, $\delta = 0.5$ nm, $pK_a = 8.3$, $\varepsilon = 80$, and $\Gamma_0 = 4.7 \times 10^{18}$ m^{-2}.)

particles tend to aggregate. For pH 9.3 (Figure 3b), however, the interparticle potential becomes repulsive and the particles disperse.

When bulk NP oscillations are coupled to transport or surface phenomena, they can give rise to various spatiotemporal phenomena and patterns. For example, when a homogeneous mixture of the MGSG reactants and aggregated NPs is placed in an unstirred tube, the free liquid/air interface initiates an autocatalytic front of NP deaggregation/color change that propagates along the tube with a velocity of about 1.5 cm s^{-1} (Figure 4a; Supporting Information, Movie 4). The mechanism of this front propagation is analogous to that described for molecular systems,[40] and the fact that it starts near the interface is due to interfacial fluctuations. In a potentially more practical example, NP oscillations can drive surface deposition and cleaning of nanoparticles. This is illustrated in Figure 4b, which shows a biphasic toluene/water system in which the FMP-coated NPs can reside either at the liquid–liquid interface or can wet and deposit on the glass walls of the container. As we described elsewhere,[41] the

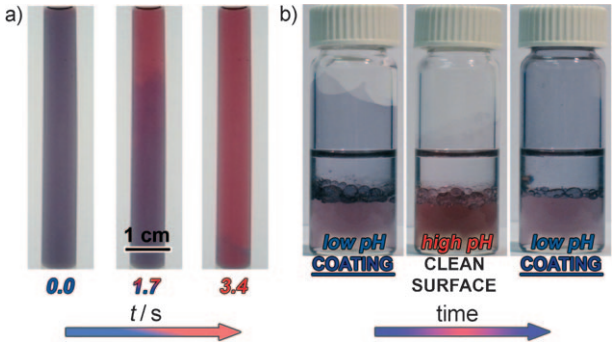

Figure 4. Nanoparticle front propagation and surface coating/cleaning. a) A pH front propagating down a test-tube causes dispersion of the initially aggregated Au NPs. The tube contains 0.5 mM Au NPs and the components of the methylene glycol/sulfite/gluconolactone system ([SO_3^{2-}] = 0.005 M, [HSO_3^-] = 0.05 M, [formaldehyde] = 0.1 M, [gluconolactone] = 0.0067 M). Purple and red colors correspond to aggregated and unaggregated Au NPs, respectively. b) Au NPs coated with FMP ligands periodically coat (blue film) and clean (clear surface) the walls of a glass vial containing a biphasic water/toluene mixture (2 mL:1.25 mL). This rhythmic process is driven by the pH oscillations occurring in the aqueous phase. Composition of the pH oscillator: [SO_3^{2-}] = 0.005 M, [HSO_3^-] = 0.05 M, [formaldehyde] = 0.1 M, [gluconolactone] = 0.0067 M, [Au NP] = 0.4 mM.

preference for either of these locations depends, to the first approximation, on the pH; when the FMP ligands on the particles are protonated, these NPs prefer to deposit onto the walls of the container; when the ligands are deprotonated, the particles prefer the liquid–liquid interface. Not surprisingly, when this system is coupled to the pH oscillations in the aqueous phase, the NPs rhythmically deposit on the glass walls and then wash away from them.

In summary, we demonstrated that chemical oscillations can translate into and can control rhythmic aggregation of nanoscopic particles. As these phenomena derive from relatively simple balance between vdW and charge–charge interactions, it should be possible to extend them to other charged nanoscale entities, including biological compounds such as DNA or proteins (though, in such cases, the range of pH should be adjusted carefully to prevent denaturation). In a wider context, control of nanoscale systems by nonlinear chemical kinetics could open new avenues for research on dynamic/non-equilibrium nanostructured materials.[3,4,10,11]

Received: July 11, 2010
Published online: September 30, 2010

Keywords: front propagation · nanoparticles · nonlinear chemical dynamics · oscillations · self-assembly

[1] J. van de Koppel, J. C. Gascoigne, G. Theraulaz, M. Rietkerk, W. M. Mooij, P. M. J. Herman, *Science* **2008**, *322*, 739–742.
[2] S. Soh, M. Byrska, K. Kandere-Grzybowska, B. A. Grzybowski, *Angew. Chem.* **2010**, *122*, 4264–4294; *Angew. Chem. Int. Ed.* **2010**, *49*, 4170–4198.
[3] M. Fialkowski, K. J. M. Bishop, R. Klajn, S. K. Smoukov, C. J. Campbell, B. A. Grzybowski, *J. Phys. Chem. B* **2006**, *110*, 2482–2496.
[4] B. A. Grzybowski, C. E. Wilmer, J. Kim, K. Browne, K. J. M. Bishop, *Soft Matter* **2009**, *5*, 1110–1128.
[5] I. R. Epstein, K. Showalter, *J. Phys. Chem.* **1996**, *100*, 13132–13147.
[6] I. R. Epstein, J. A. Pojman, *An Introduction to Nonlinear Chemical Dynamics: oscillations, waves, patterns, and chaos*, Oxford University Press, Oxford, **1998**, p. 392.
[7] R. E. Liesegang, *Naturwiss. Wochenschr.* **1896**, *11*, 353–362.
[8] V. Castets, E. Dulos, J. Boissonade, P. De Kepper, *Phys. Rev. Lett.* **1990**, *64*, 2953–2956.
[9] J. Horváth, I. Szalai, P. De Kepper, *Science* **2009**, *324*, 772–775.
[10] R. Klajn, P. J. Wesson, K. J. M. Bishop, B. A. Grzybowski, *Angew. Chem.* **2009**, *121*, 7169–7173; *Angew. Chem. Int. Ed.* **2009**, *48*, 7035–7039.
[11] Y. Wei, S. Han, J. Kim, S. Soh, B. A. Grzybowski, *J. Am. Chem. Soc.* **2010**, *132*, 11018–11020.
[12] E. Rabani, D. R. Reichman, P. L. Geissler, L. E. Brus, *Nature* **2003**, *426*, 271–274.
[13] S. A. Jenekhe, X. L. Chen, *Science* **1999**, *283*, 372–375.
[14] A. B. Subramaniam, M. Abkarian, H. A. Stone, *Nat. Mater.* **2005**, *4*, 553–556.
[15] G. M. Whitesides, B. Grzybowski, *Science* **2002**, *295*, 2418–2421.
[16] G. M. Whitesides, M. Boncheva, *Proc. Natl. Acad. Sci. USA* **2002**, *99*, 4769–4774.
[17] I. Varga, I. Szalai, R. Mészáros, T. Gilányi, *J. Phys. Chem. B* **2006**, *110*, 20297–20301.
[18] R. Yoshida, T. Takahashi, T. Yamaguchi, H. Ichijo, *J. Am. Chem. Soc.* **1996**, *118*, 5134–5135.

[19] K. Kurin-Csörgei, I. R. Epstein, M. Orbán, *Nature* **2005**, *433*, 139 – 142.
[20] K. Kurin-Csörgei, I. R. Epstein, M. Orbán, *J. Phys. Chem. A* **2006**, *110*, 7588 – 7592.
[21] K. Kovács, M. Leda, V. K. Vanag, I. R. Epstein, *J. Phys. Chem. A* **2009**, *113*, 146 – 156.
[22] V. Horváth, K. Kurin-Csörgei, I. R. Epstein, M. Orbán, *Phys. Chem. Chem. Phys.* **2010**, *12*, 1248 – 1252.
[23] X. Han, Y. Li, S. Wu, Z. Deng, *Small* **2008**, *4*, 326 – 329.
[24] R. McIlwaine, K. Kovács, S. K. Scott, A. F. Taylor, *Chem. Phys. Lett.* **2006**, *417*, 39 – 42.
[25] K. Kovács, R. E. McIlwaine, S. K. Scott, A. F. Taylor, *J. Phys. Chem. A* **2007**, *111*, 549 – 551.
[26] K. Kovács, R. E. McIlwaine, S. K. Scott, A. F. Taylor, *Phys. Chem. Chem. Phys.* **2007**, *9*, 3711 – 3716.
[27] K. J. M. Bishop, C. E. Wilmer, S. Soh, B. A. Grzybowski, *Small* **2009**, *5*, 1600 – 1630.
[28] J. C. Love, L. A. Estroff, J. K. Kriebel, R. G. Nuzzo, G. M. Whitesides, *Chem. Rev.* **2005**, *105*, 1103 – 1170.
[29] D. Witt, R. Klajn, P. Barski, B. A. Grzybowski, *Curr. Org. Chem.* **2004**, *8*, 1763 – 1797.
[30] K. J. M. Bishop, B. A. Grzybowski, *ChemPhysChem* **2007**, *8*, 2171 – 2176.
[31] The ratio of the magnitudes of vdW and electrostatic energies increases with NP radius; for water-soluble particles with diameters in tens of nm, the attractions always dominate, causing irreversible NP aggregation.
[32] A. M. Kalsin, B. Kowalczyk, S. K. Smoukov, R. Klajn, B. A. Grzybowski, *J. Am. Chem. Soc.* **2006**, *128*, 15046 – 15047.
[33] S. Hay, K. Westerlund, C. Tommos, *Biochemistry* **2005**, *44*, 11891 – 11902.
[34] D. Wang, B. Kowalczyk, I. Lagzi, B. A. Grzybowski, *J. Phys. Chem. Lett.* **2010**, *1*, 1459 – 1462.
[35] A. O. Pinchuk, A. M. Kalsin, B. Kowalczyk, G. C. Schatz, B. A. Grzybowski, *J. Phys. Chem. C* **2007**, *111*, 11816 – 11822.
[36] A. M. Kalsin, A. O. Pinchuk, S. K. Smoukov, M. Paszewski, G. C. Schatz, B. A. Grzybowski, *Nano Lett.* **2006**, *6*, 1896 – 1903.
[37] K. J. M. Bishop, B. Kowalczyk, B. A. Grzybowski, *J. Phys. Chem. B* **2009**, *113*, 1413 – 1417.
[38] V. A. Parsegian, G. H. Weiss, *J. Colloid Interface Sci.* **1981**, *81*, 285 – 289.
[39] B. W. Ninhama, *Adv. Colloid Interface Sci.* **1999**, *83*, 1 – 17.
[40] K. Showalter, J. J. Tyson, *J. Chem. Educ.* **1987**, *64*, 742 – 744.
[41] B. Kowalczyk, M. M. Apodaca, S. Soh, B. A. Grzybowski, *Langmuir* **2009**, *25*, 12855 – 12859.

